PERGAMON

International Journal of Heat and Mass Transfer 42 (1999) 219–229

International Journal of HEAT and MASS TRANSFER

Three-dimensional propagation of hyperbolic thermal waves in a solid bar with rectangular cross-section

A. Barletta*, E. Zanchini

Dipartimento di Ingegneria Energetica, Nucleare e del Controllo Ambientale (DIENCA), Università di Bologna, Viale Risorgimento 2, I-40136 Bologna, Italy

Received 14 April 1998

Abstract

The hyperbolic heat conduction in a solid bar with a rectangular section is analyzed. Each surface of the bar is subjected to a uniform and time varying heat flux. It is shown that, according to the heat-flux formulation of hyperbolic heat conduction, the heat flux density field can be determined by employing the analytical solution of a one-dimensional problem. The distributions of the heat flux density and the temperature are obtained for a bar with a finite length and with arbitrary time-evolutions of the heat flux on its surfaces. Special attention is devoted to a two-dimensional case, i.e. that of a bar with insulated ends. In this case, plots of the temperature field at given instants of time are reported and compared with those which correspond to a vanishing relaxation time.

Key words: Heat conduction; Thermal waves; Relaxation time

Nomenclature

a_i for $i = 1, 2, 3$, dimensionless functions of ξ, η and Λ defined by equation (39)
b dimensionless function of ξ, η and Λ defined by equation (44)
c specific heat
erfc complementary error function
f dimensionless function of ω, η and Λ defined by equations (35) and (37)
$F_0^{(i)}$ for $i = 1, 2, 3$, arbitrary dimensionless functions of time
$F_L^{(i)}$ for $i = 1, 2, 3$, arbitrary dimensionless functions of time
g dimensionless function of ξ, η and Λ defined by equation (33)
I_v modified Bessel function of first kind and order v
k thermal conductivity
L_i for $i = 1, 2, 3$, lengths of bar edges
$\mathscr{L}^{-1}$ inverse Laplace transform operator
n non-negative integer
$N_{\max}$ the smallest non-negative integer such that equation (36) holds
p Laplace transform variable
$\mathbf{q}$ heat flux density
q_i for $i = 1, 2, 3$, components of $\mathbf{q}$ along the axes x_1, x_2, x_3
t time
T temperature
T_0 temperature for $t = 0$
u internal energy per unit mass
U Heaviside's unit step function
w power generated per unit volume
$\mathbf{x}$ position vector
x_i for $i = 1, 2, 3$, spatial coordinates
Y, Z dimensionless coordinates defined by equation (42).

Greek symbols

α $= k/(\rho c)$, thermal diffusivity
β dimensionless parameter defined by equation (31)
η dimensionless time defined by equation (22)
θ dimensionless temperature defined by equation (42)
λ dummy integration variable employed in equation (32)

* Corresponding author. Tel.: 00 39 51 6443295; Fax: 00 39 51 6443296; E-mail: antonio.barletta@mail.ing.unibo.it

0017–9310/98/$—see front matter
PII: S0017–9310(98)00190–2

Λ dimensionless parameter defined by equation (22)
μ dimensionless function of ω, η and Λ defined by equations (46) and (48)
ξ dimensionless coordinate defined by equation (22)
Ξ dimensionless parameter defined by equation (42)
ρ mass density
σ aspect ratio defined by equation (42)
τ thermal relaxation time
ϕ_i for $i = 1, 2, 3$, dimensionless heat fluxes defined by equation (23)
φ dimensionless function of ω, η and Λ defined by equation (47)
χ dimensionless time defined by equation (42)
$\psi_0^{(i)}$ for $i = 1, 2, 3$, dimensionless functions of η defined by equation (23)
$\psi_1^{(i)}$ for $i = 1, 2, 3$, dimensionless functions of η defined by equation (23)
ω dimensionless variable employed in equations (35), (37) and (46)–(48).

Superscripts and subscripts
$\sim$ Laplace transformed function
$'$ dummy integration variable.

1. Introduction

In the last decades, several experiments have shown that the classical theory of heat conduction in solids based on Fourier's law

$$\mathbf{q} = -k\nabla T \tag{1}$$

may fail when unsteady processes with rapid changes of the temperature and of the heat flux are involved. Indeed, equation (1) when combined with the local energy balance equation

$$\nabla\cdot\mathbf{q} + \rho\frac{\partial u}{\partial t} = w \tag{2}$$

and with the relation $\mathrm{d}u = c\,\mathrm{d}T$ leads, for a solid with constant values of ρ, c and k, to the differential equation

$$\rho c\frac{\partial T}{\partial t} = k\nabla^2 T + w. \tag{3}$$

Equation (3) is a parabolic partial-differential equation and implies an infinite propagation speed of the temperature signal. This property of Fourier's theory conflicts with several experiments performed both at very low temperatures, as for instance the experiment by Ackerman and Guyer in solid helium [1], and at room temperatures, as the experiment by Kaminski [2] and that by Mitra et al. [3]. In order to obtain a theory of heat conduction compatible with a finite propagation speed of thermal signals, Cattaneo [4, 5] and Vernotte [6, 7] proposed a modification of Fourier's law, which is now well known as Cattaneo–Vernotte's constitutive equation

$$\mathbf{q} + \tau\frac{\partial \mathbf{q}}{\partial t} = -k\nabla T. \tag{4}$$

If equation (4) is combined with equation (2) and with the relation $\mathrm{d}u = c\,\mathrm{d}T$, one obtains for a solid with constant values of ρ, c and k,

$$\rho c\left(\frac{\partial T}{\partial t} + \tau\frac{\partial^2 T}{\partial t^2}\right) = k\nabla^2 T + w + \tau\frac{\partial w}{\partial t}. \tag{5}$$

Equation (5) is a hyperbolic partial-differential equation and yields a finite value, $\sqrt{\alpha/\tau}$, for the propagation speed of the temperature signals. Obviously, in the limit $\tau \to 0$, equation (5) tends to equation (3) and the propagation speed $\sqrt{\alpha/\tau}$ tends to infinity.

Many solutions of equation (5) have been obtained in several papers available in the literature. Most of them analyze one-dimensional cases and deal either with plane slabs or with semi-infinite media bounded by a plane surface. A wide list of these papers can be found in the review by Ozisik and Tzou [8]. The literature on one-dimensional propagation of thermal waves in cylindrical domains is less abundant [9–14].

Few papers analyze hyperbolic heat conduction in two or three dimensions. To the authors' knowledge, all the solutions available in the literature in more than one dimension are obtained by employing numerical methods. Yang [15] describes a high-resolution numerical method for the analysis of hyperbolic heat conduction in two-dimensional domains. Chen and Lin [16, 17] present illustrative examples of thermal-wave propagation in two dimensions. These authors solve equation (5) by the following numerical procedure. First, the Laplace transform technique is employed to remove the time derivatives from equation (5). Then, the discretized equation in the transform domain is solved by the control volume method.

In the present paper, an analytical expression of the temperature field is obtained for a three-dimensional problem of hyperbolic heat conduction. In particular, the propagation of thermal waves in a finite bar with a rectangular cross-section is analyzed in the case of unsteady and uniform heat fluxes on the six boundary surfaces. The heat-flux formulation results to be particularly convenient in this case. In fact, the solution of the three-dimensional problem is easily obtained by employing the solution of an auxiliary one-dimensional problem. The latter is solved by means of the Laplace transform technique. A detailed analysis is presented for the special case of a bar with insulated ends.

2. The heat-flux formulation

In this section, the heat-flux formulation of hyperbolic heat conduction is outlined. Then, it is shown that the

three components of the heat flux density fulfil three partial-differential equations which may be solved separately.

The heat-flux formulation of hyperbolic heat conduction based on Cattaneo–Vernotte's constitutive equation is described in the paper by Frankel et al. [18]. This formulation of hyperbolic heat conduction is based on the partial-differential equation satisfied by the heat flux density $\mathbf{q}$

$$\alpha[\nabla(\nabla\cdot\mathbf{q})-\nabla w]=\frac{\partial\mathbf{q}}{\partial t}+\tau\frac{\partial^2\mathbf{q}}{\partial t^2}. \tag{6}$$

Equation (6) is easily obtained by combining equation (4) with equation (2) and with the relation $\mathrm{d}u=c\,\mathrm{d}T$, for a solid with constant values of ρ, c, k and τ.

In the following, it will be shown that, if $\nabla\times\mathbf{q}=0$ for $t=0$, equation (6) can be expressed in a simpler form. On account of the vector identity [19]

$$\nabla(\nabla\cdot\mathbf{q})=\nabla^2\mathbf{q}+\nabla\times(\nabla\times\mathbf{q}) \tag{7}$$

equation (6) can be rewritten as

$$\alpha[\nabla^2\mathbf{q}+\nabla\times(\nabla\times\mathbf{q})-\nabla w]=\frac{\partial\mathbf{q}}{\partial t}+\tau\frac{\partial^2\mathbf{q}}{\partial t^2}. \tag{8}$$

If the thermal relaxation time τ is nonzero, equation (4) implies the relation

$$\frac{\partial}{\partial t}(\mathrm{e}^{t/\tau}\mathbf{q})=-\frac{k}{\tau}\nabla(\mathrm{e}^{t/\tau}T). \tag{9}$$

As a consequence of equation (9), one obtains

$$\frac{\partial}{\partial t}(\mathrm{e}^{t/\tau}\nabla\times\mathbf{q})=0. \tag{10}$$

Therefore, $\nabla\times\mathbf{q}$ can be expressed as

$$\nabla\times\mathbf{q}(\mathbf{x},t)=\mathrm{e}^{-t/\tau}\nabla\times\mathbf{q}(\mathbf{x},0) \tag{11}$$

so that, if $\nabla\times\mathbf{q}$ is zero for $t=0$, it is zero for every $t>0$. In this case, equation (8) yields

$$\alpha[\nabla^2\mathbf{q}-\nabla w]=\frac{\partial\mathbf{q}}{\partial t}+\tau\frac{\partial^2\mathbf{q}}{\partial t^2}. \tag{12}$$

Indeed, the constraint $\nabla\times\mathbf{q}=0$ for $t=0$ is a restriction not so severe as it seems, for the following reason. Usually, the initial state of a non-stationary heat conduction problem is either a thermodynamic equilibrium state or, at least, a steady state. In the former case, $\mathbf{q}(\mathbf{x},0)$ is zero and, as a consequence, is irrotational. In the latter case, $\partial\mathbf{q}(\mathbf{x},0)/\partial t$ is zero, so that for $t=0$ equation (4) coincides with equation (1). If equation (1) holds at $t=0$ and k is a constant, $\mathbf{q}(\mathbf{x},0)$ is irrotational. It should be pointed out that, unlike equation (6), equation (12) yields no interaction between the components of $\mathbf{q}$. Indeed, equation (12) can be split into the three scalar equations

$$\alpha\left[\nabla^2 q_1-\frac{\partial w}{\partial x_1}\right]=\frac{\partial q_1}{\partial t}+\tau\frac{\partial^2 q_1}{\partial t^2} \tag{13}$$

$$\alpha\left[\nabla^2 q_2-\frac{\partial w}{\partial x_2}\right]=\frac{\partial q_2}{\partial t}+\tau\frac{\partial^2 q_2}{\partial t^2} \tag{14}$$

$$\alpha\left[\nabla^2 q_3-\frac{\partial w}{\partial x_3}\right]=\frac{\partial q_3}{\partial t}+\tau\frac{\partial^2 q_3}{\partial t^2}. \tag{15}$$

In principle, equations (13)–(15) imply that the three components q_1, q_2 and q_3 are independent variables. However, an interaction between q_1, q_2 and q_3 can be induced by the boundary conditions. For instance, if the boundary temperature is prescribed, the energy balance equation

$$\nabla\cdot\mathbf{q}+\rho c\frac{\partial T}{\partial t}=w \tag{16}$$

implies that a constraint on $\nabla\cdot\mathbf{q}$ is present at the boundary. In this case, q_1, q_2 and q_3 cannot be considered as independent. On the other hand, if the boundary heat flux is prescribed, q_1, q_2 and q_3 can be determined separately. A three-dimensional problem of this kind will be analyzed in the forthcoming section.

According to the heat-flux formulation of hyperbolic heat conduction, when the heat flux density $\mathbf{q}$ has been obtained by solving equations (13)–(15), the temperature distribution can be evaluated by employing equation (16), i.e.

$$T(\mathbf{x},t)=T(\mathbf{x},0)-\frac{1}{\rho c}\int_0^t[\nabla\cdot\mathbf{q}(\mathbf{x},t')-w(\mathbf{x},t')]\,\mathrm{d}t'. \tag{17}$$

3. A three-dimensional problem

In this section, the heat-flux formulation is employed in the analysis of hyperbolic heat conduction in a bar with a rectangular cross section and with a finite length.

Let us consider a bar with a length L_1 and a rectangular cross section with sides L_2 and L_3. A drawing of the bar and of the coordinate system is reported in Fig. 1. The bar has constant values of the mass density ρ, of the thermal conductivity k, of the specific heat c and of the thermal relaxation time τ. Moreover, no internal heat generation occurs within the bar, so that $w=0$. Each surface of the bar is subjected to a uniform and non-stationary heat flux density, namely

$$q_1(0,x_2,x_3,t)=q_0F_0^{(1)}(t),\quad q_1(L_1,x_2,x_3,t)=-q_0F_L^{(1)}(t) \tag{18}$$

$$q_2(x_1,0,x_3,t)=q_0F_0^{(2)}(t),\quad q_2(x_1,L_2,x_3,t)=-q_0F_L^{(2)}(t) \tag{19}$$

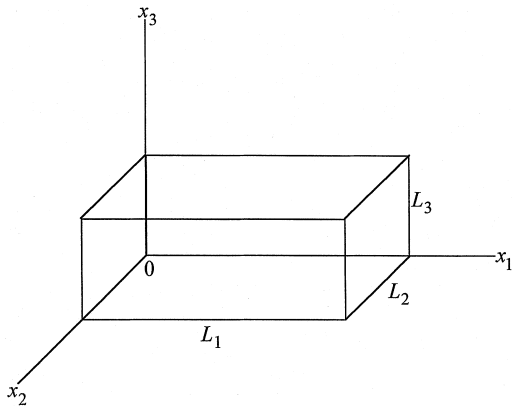

Fig. 1. Drawing of the bar and of the coordinate system.

$$q_3(x_1, x_2, 0, t) = q_0 F_0^{(3)}(t), \quad q_3(x_1, x_2, L_3, t) = -q_0 F_L^{(3)}(t) \tag{20}$$

where the functions $F_0^{(i)}(t)$ and $F_L^{(i)}(t)$, for $i = 1, 2, 3$, are prescribed dimensionless functions of t. The initial conditions are

$$\mathbf{q}(x_1, y_2, z_3, 0) = 0, \quad T(x_1, y_2, z_3, 0) = T_0. \tag{21}$$

On account of equation (4), equation (21) ensures that $\partial \mathbf{q}/\partial t = 0$ for $t = 0$. Moreover, equations (11) and (21) imply that $\nabla \times \mathbf{q} = 0$ at every instant of time, so that equations (13)–(15) hold. Obviously, equations (13)–(15), together with the boundary conditions (18)–(20) and the initial condition (21), yield no interaction between q_1, q_2 and q_3. In other words, each of the components q_1, q_2 and q_3 can be determined separately. On account of equations (13)–(15) and (18)–(20), one can conclude that q_1 depends only on x_1 and t, q_2 depends only on x_2 and t, q_3 depends only on x_3 and t. Thus, each q_i, for $i = 1, 2, 3$, is the solution of a one-dimensional heat conduction problem.

4. An auxiliary one-dimensional problem

In this section, the distribution of the heat flux density and the temperature field within the bar described in the preceding section are obtained by means of an auxiliary one-dimensional boundary value problem, which is solved by the Laplace transform method.

For $i = 1, 2, 3$, let us define the dimensionless quantities

$$\xi = \frac{x_i}{L_i}, \quad \eta = \frac{\alpha t}{L_i^2}, \quad \Lambda = \frac{\alpha \tau}{L_i^2} \tag{22}$$

and the dimensionless functions

$$\phi_i(\xi, \eta, \Lambda) = \frac{q_i\left(L_i\xi, \dfrac{L_i^2\eta}{\alpha}\right)}{q_0}, \quad \psi_0^{(i)}(\eta) = F_0^{(i)}\left(\frac{L_i^2\eta}{\alpha}\right),$$

$$\psi_1^{(i)}(\eta) = F_L^{(i)}\left(\frac{L_i^2\eta}{\alpha}\right). \tag{23}$$

On account of equations (22) and (23), equations (13)–(15) and (18)–(21) yield

$$\frac{\partial^2 \phi_i}{\partial \xi^2} = \frac{\partial \phi_i}{\partial \eta} + \Lambda \frac{\partial^2 \phi_i}{\partial \eta^2} \tag{24}$$

$$\phi_i(0, \eta, \Lambda) = \psi_0^{(i)}(\eta), \quad \phi_i(1, \eta, \Lambda) = -\psi_1^{(i)}(\eta) \tag{25}$$

$$\phi_i(\xi, 0, \Lambda) = 0, \quad \left.\frac{\partial \phi_i(\xi, \eta, \Lambda)}{\partial \eta}\right|_{\eta = 0} = 0. \tag{26}$$

Equations (24)–(26) can be solved by the Laplace transform method. The transform of $\phi_i(\xi, \eta, \Lambda)$ is given by

$$\tilde{\phi}_i(\xi, p, \Lambda) = \int_0^\infty \mathrm{e}^{-p\eta} \phi_i(\xi, \eta, \Lambda)\, \mathrm{d}\eta. \tag{27}$$

On account of the properties of Laplace transforms [20], equations (24) and (26) yield

$$\frac{\partial^2 \tilde{\phi}_i}{\partial \xi^2} = (p + \Lambda p^2)\tilde{\phi}_i \tag{28}$$

while equation (25) can be rewritten as

$$\tilde{\phi}_i(0, p, \Lambda) = \tilde{\psi}_0^{(i)}(p), \quad \tilde{\phi}_i(1, p, \Lambda) = -\tilde{\psi}_1^{(i)}(p). \tag{29}$$

The solution of equations (28) and (29) can be expressed as

$$\tilde{\phi}_i(\xi, p, \Lambda) = \tilde{\psi}_0^{(i)}(p) \frac{\sinh[\beta(1-\xi)]}{\sinh(\beta)} - \tilde{\psi}_1^{(i)}(p) \frac{\sinh(\beta\xi)}{\sinh(\beta)} \tag{30}$$

where

$$\beta = (p + \Lambda p^2)^{1/2}. \tag{31}$$

Then, on account of the convolution theorem for Laplace transforms [20], equation (30) yields

$$\phi_i(\xi, \eta, \Lambda) = \int_0^\eta \left[\frac{\mathrm{d}\psi_0^{(i)}(\lambda)}{\mathrm{d}\lambda} g(1-\xi, \eta-\lambda, \Lambda) - \frac{\mathrm{d}\psi_1^{(i)}(\lambda)}{\mathrm{d}\lambda} g(\xi, \eta-\lambda, \Lambda) \right] \mathrm{d}\lambda \tag{32}$$

where $g(\xi, \eta, \Lambda)$ is the inverse transform of the function

$$\tilde{g}(\xi, p, \Lambda) = \frac{\sinh(\beta\xi)}{p \sinh(\beta)}. \tag{33}$$

As is shown in the Appendix, $g(\xi,\eta,\Lambda)$ can be expressed as

$$g(\xi,\eta,\Lambda)=\sum_{n=0}^{N_{\max}}[f(2n+1-\xi,\eta,\Lambda)-f(2n+1+\xi,\eta,\Lambda)] \tag{34}$$

where, if $\Lambda\neq 0$, $f(\omega,\eta,\Lambda)$ is given by

$$f(\omega,\eta,\Lambda)=U(\eta-\omega\sqrt{\Lambda})\left[\mathrm{e}^{-\omega/(2\sqrt{\Lambda})}+\frac{\omega}{2\sqrt{\Lambda}}\int_{\omega\sqrt{\Lambda}}^{\eta}\frac{\mathrm{e}^{-\eta'/(2\Lambda)}}{\sqrt{\eta'^2-\omega^2\Lambda}}\times I_1\left(\frac{1}{2\Lambda}\sqrt{\eta'^2-\omega^2\Lambda}\right)\mathrm{d}\eta'\right] \tag{35}$$

and $N_{\max}$ is the smallest non-negative integer such that

$$N_{\max}\geqslant\frac{1}{2}\left(\frac{\eta}{\sqrt{\Lambda}}-1+\xi\right). \tag{36}$$

On the other hand, if $\Lambda=0$, $f(\omega,\eta,0)$ is given by

$$f(\omega,\eta,0)=\mathrm{erfc}\left(\frac{\omega}{2\sqrt{\eta}}\right) \tag{37}$$

while $N_{\max}=+\infty$.

On account of equations (17), (22) and (23), the temperature field for the three-dimensional case can be expressed as

$$T(\mathbf{x},t)=T_0-\frac{q_0}{\rho c}\int_0^t\sum_{i=1}^{3}\frac{1}{L_i}a_i\left(\frac{x_i}{L_i},\frac{\alpha t'}{L_i^2},\frac{\alpha\tau}{L_i^2}\right)\mathrm{d}t' \tag{38}$$

where, for $i=1, 2, 3$,

$$a_i(\xi,\eta,\Lambda)=\frac{\partial\phi_i(\xi,\eta,\Lambda)}{\partial\xi}. \tag{39}$$

To summarize, for any arbitrary choice of the dimensionless functions $F_0^{(i)}(t)$ and $F_L^{(i)}(t)$, with $i=1, 2, 3$, the temperature field within the bar can be determined by employing equations (23), (32) and (34)–(39).

5. A bar with insulated ends

In this section, the expression of the temperature field obtained for the three-dimensional conduction in a bar with prescribed boundary heat fluxes is applied to a special case: a bar with insulated ends.

Let us consider the bar described in the preceding sections and assume that the surfaces $x_1=0$ and $x_1=L_1$ are insulated, i.e. that $F_0^{(1)}(t)$ and $F_L^{(1)}(t)$ are zero. As a consequence of equations (23), (32) and (39), one can conclude that, in this case, both $\phi_1(\xi,\eta,\Lambda)$ and $a_1(\xi,\eta,\Lambda)$ are zero. Therefore, equation (38) ensures that the temperature does not depend on x_1, so that the heat conduction is two-dimensional. Indeed, if the ends are insulated, the temperature distribution is the same which would occur for a bar with an infinite length.

Let us assume that the same constant heat flux density is prescribed on the non-insulated boundary surfaces, namely

$$F_0^{(2)}(t)=F_0^{(3)}(t)=F_L^{(2)}(t)=F_L^{(3)}(t)=U(t). \tag{40}$$

In this case, equation (32) yields, for $i=2, 3$,

$$\phi_i(\xi,\eta,\Lambda)=g(1-\xi,\eta,\Lambda)-g(\xi,\eta,\Lambda). \tag{41}$$

Let us define the dimensionless quantities

$$Y=\frac{x_2}{L_2},\quad Z=\frac{x_3}{L_2},\quad \chi=\frac{\alpha t}{L_2^2},\quad \Xi=\frac{\alpha\tau}{L_2^2}$$
$$\sigma=\frac{L_3}{L_2},\quad \theta=k\frac{T-T_0}{q_0L_2}. \tag{42}$$

Equations (38) and (42) yield

$$\theta(Y,Z,\chi)=b(1-Y,\chi,\Xi)+b(Y,\chi,\Xi)+\sigma[b(1-Z/\sigma,\chi/\sigma^2,\Xi/\sigma^2)+b(Z/\sigma,\chi/\sigma^2,\Xi/\sigma^2)] \tag{43}$$

where $b(\xi,\eta,\Lambda)$ is defined as

$$b(\xi,\eta,\Lambda)=\int_0^{\eta}\frac{\partial g(\xi,\eta',\Lambda)}{\partial\xi}\mathrm{d}\eta'. \tag{44}$$

On account of equations (34), (35) and (37), the function $b(\xi,\eta,\Lambda)$ is given by

$$b(\xi,\eta,\Lambda)=\sum_{n=0}^{N_{\max}}[\mu(2n+1-\xi,\eta,\Lambda)+\mu(2n+1+\xi,\eta,\Lambda)] \tag{45}$$

where, if $\Lambda\neq 0$, the function $\mu(\omega,\eta,\Lambda)$ can be expressed as

$$\mu(\omega,\eta,\Lambda)=U(\eta-\omega\sqrt{\Lambda})[\sqrt{\Lambda}\,\mathrm{e}^{-\omega/(2\sqrt{\Lambda})}-\int_{\omega\sqrt{\Lambda}}^{\eta}\varphi(\omega,\eta',\Lambda)\,\mathrm{d}\eta']. \tag{46}$$

The function $\varphi(\omega,\eta,\Lambda)$ employed in equation (46) is defined as

$$\varphi(\omega,\eta,\Lambda)=-\frac{\omega+4\sqrt{\Lambda}}{8\Lambda}\mathrm{e}^{-\omega/(2\sqrt{\Lambda})}$$

$$+\frac{1}{2\sqrt{\Lambda}}\int_{\omega\sqrt{\Lambda}}^{\eta} e^{-\eta'/(2\Lambda)}\left[\frac{I_1\left(\frac{1}{2\Lambda}\sqrt{\eta'^2-\omega^2\Lambda}\right)}{\sqrt{\eta'^2-\omega^2\Lambda}}\right.$$

$$\left.-\frac{\omega^2}{2}\frac{I_2\left(\frac{1}{2\Lambda}\sqrt{\eta'^2-\omega^2\Lambda}\right)}{\eta'^2-\omega^2\Lambda}\right]d\eta'. \quad (47)$$

On the other hand, $\mu(\omega,\eta,0)$ is given by

$$\mu(\omega,\eta,0)=2\sqrt{\frac{\eta}{\pi}}e^{-\omega^2/(4\eta)}-\omega\,\mathrm{erfc}\left(\frac{\omega}{2\sqrt{\eta}}\right). \quad (48)$$

For arbitrarily chosen values of the dimensionless parameters Ξ and σ, equations (43) and (45)–(48) allow one to evaluate the dimensionless temperature field $\theta(Y,Z,\chi)$.

6. Discussion of the results

Figures 2–5 refer to a bar with insulated ends and with $L_2=L_3$, i.e. with $\sigma=1$. In particular, Figs 2 and 4 present plots of the dimensionless temperature θ as a function of Y and Z, for $\Xi=1$. These plots refer to $\chi=0.25$ and $\chi=0.75$, respectively. Figures 2 and 4 display the distribution of θ in the region with $0\leqslant Y\leqslant 0.5$ and $0\leqslant Z\leqslant 0.5$. On account of the symmetry of the bar and of the boundary conditions, the behaviour of θ in the whole section of the bar is easily inferred from Figs 2 and 4. Figure 2 shows that, when $\chi=0.25$, the temperature signal has not yet reached the internal region with $0.25\leqslant Y\leqslant 0.75$ and $0.25\leqslant Z\leqslant 0.75$. An interference between the wavefronts generated on the boundary planes $Y=0$ and $Z=0$ is present in the region with $0\leqslant Y\leqslant 0.25$ and $0\leqslant Z\leqslant 0.25$. In this region, the higher values of θ are caused by the overlap of the temperature signals which propagate in the Y-direction and in the Z-direction.

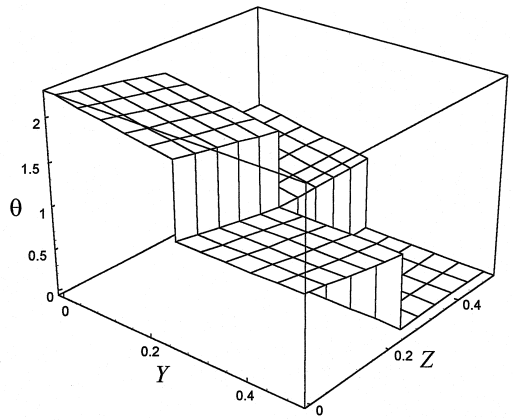

Fig. 2. Plot of the dimensionless temperature θ as a function of Y and Z for $\chi=0.25$, $\sigma=1$ and $\Xi=1$.

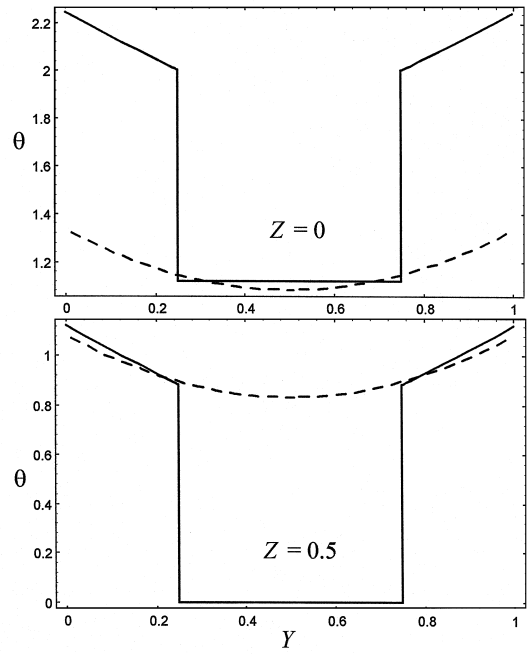

Fig. 3. Plots of θ vs. Y at $Z=0$ and at $Z=0.5$ for $\chi=0.25$ and $\sigma=1$. The solid lines refer to $\Xi=1$, while the dashed lines refer to $\Xi=0$.

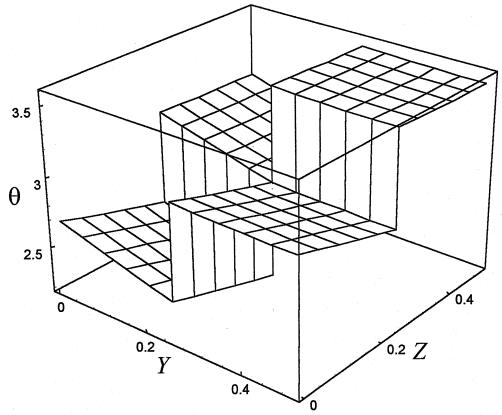

Fig. 4. Plot of the dimensionless temperature θ as a function of Y and Z for $\chi=0.75$, $\sigma=1$ and $\Xi=1$.

Figure 3 refers to $\chi=0.25$ and presents a comparison between the behaviour of θ for $\Xi=1$ and for $\Xi=0$, both at $Z=0$ and at $Z=0.5$. The plots for $\Xi=1$ display two discontinuities of θ at $Y=0.25$ and at $Y=0.75$. Indeed, since the propagation speed of thermal signals is $\sqrt{\alpha/\tau}$, the distance spanned by the thermal wave in a dimensionless time 0.25 is given by $0.25L_2^2/\sqrt{\alpha\tau}$; if $\Xi=1$, this distance is equal to $0.25L_2$. Hence, for $\chi=0.25$ and

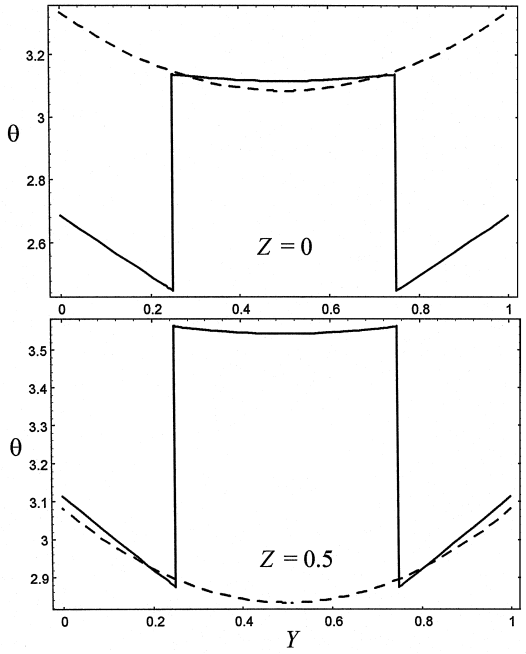

Fig. 5. Plots of θ vs. Y at $Z = 0$ and at $Z = 0.5$ for $\chi = 0.75$ and $\sigma = 1$. The solid lines refer to $\Xi = 1$, while the dashed lines refer to $\Xi = 0$.

$Z = 0$, no thermal signal travelling in the Y-direction has reached the region $0.25 \leqslant Y \leqslant 0.75$. For $\chi = 0.25$ and $Z = 0.5$, no thermal signal travelling either in the Y-direction or in the Z-direction has reached the region $0.25 \leqslant Y \leqslant 0.75$.

Figure 4 refers to $\chi = 0.75$ and $\Xi = 1$. At the dimensionless time 0.75, an interference between the temperature wavefronts generated at the four boundary planes $Y = 0$, $Y = 1$, $Z = 0$ and $Z = 1$ occurs in the internal region with $0.25 \leqslant Y \leqslant 0.75$ and $0.25 \leqslant Z \leqslant 0.75$. In this region, the thermal signals coming from the four boundary planes overlap, so that higher temperatures occur. Indeed, for $\chi = 0.75$, the temperature signals coming from the boundary have already reached the central axis of the bar, i.e. the position $Y = 0.5$ and $Z = 0.5$, and are travelling towards the boundary.

In Fig. 5, the behaviour of θ for $\Xi = 1$ is compared with the behaviour for $\Xi = 0$, at the planes $Z = 0$ and $Z = 0.5$ for $\chi = 0.75$. This figure shows that, for $\Xi = 1$ and $Z = 0$, an interference between the temperature wavefronts travelling in the Y-direction and that generated at $Z = 0$ occurs in the region $0.25 \leqslant Y \leqslant 0.75$. At $Z = 0.5$, an interference between the thermal waves travelling in the Y-direction and those travelling in the Z-direction occurs in the region $0.25 \leqslant Y \leqslant 0.75$.

Figures 6–11 refer to a bar with insulated ends and with $L_3 = 2L_2$, i.e. with $\sigma = 2$. In particular, Figs 6 and 9 present plots of the dimensionless temperature θ as a function of Y and Z for $\Xi = 1$, which refer to $\chi = 0.25$ and $\chi = 0.75$, respectively.

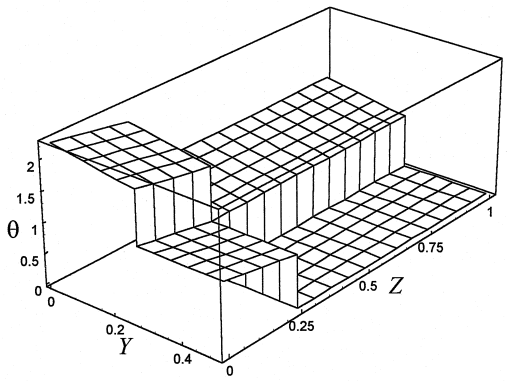

Fig. 6. Plot of the dimensionless temperature θ as a function of Y and Z for $\chi = 0.25$, $\sigma = 2$ and $\Xi = 1$.

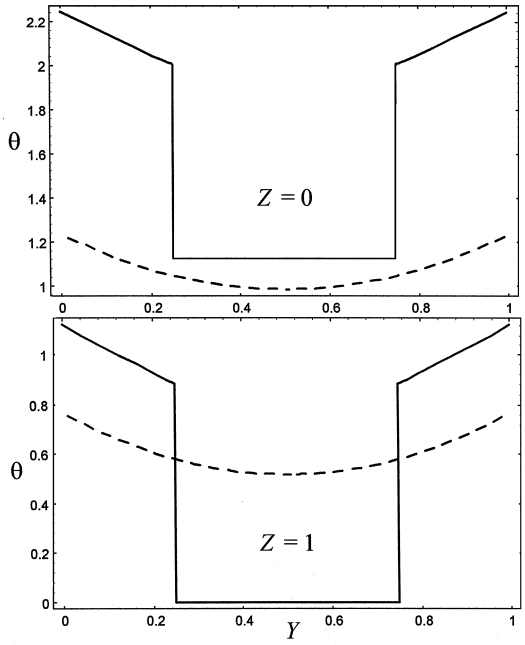

Fig. 7. Plots of θ vs. Y at $Z = 0$ and at $Z = 1$ for $\chi = 0.25$ and $\sigma = 2$. The solid lines refer to $\Xi = 1$, while the dashed lines refer to $\Xi = 0$.

Figure 6 displays an overlap between the temperature waves generated at the planes $Y = 0$ and $Z = 0$, in the region with $0 \leqslant Y \leqslant 0.25$ and $0 \leqslant Z \leqslant 0.25$. Moreover, the temperature signal has not yet reached the internal region with $0.25 \leqslant Y \leqslant 0.75$ and $0.25 \leqslant Z \leqslant 1.75$. Figures 7 and 8 refer to $\chi = 0.25$ and compare the distributions of θ for $\Xi = 1$ and for $\Xi = 0$ on the planes $Z = 0$, $Z = 1$, $Y = 0$ and $Y = 0.5$.

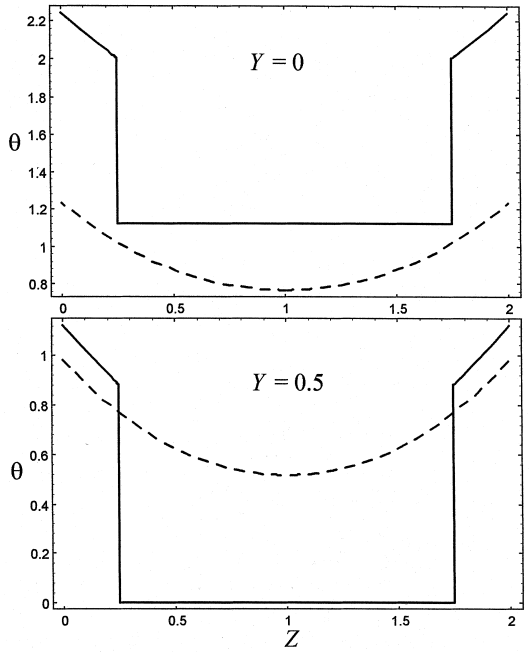

Fig. 8. Plots of θ vs. Z at $Y = 0$ and at $Y = 0.5$ for $\chi = 0.25$ and $\sigma = 2$. The solid lines refer to $\Xi = 1$, while the dashed lines refer to $\Xi = 0$.

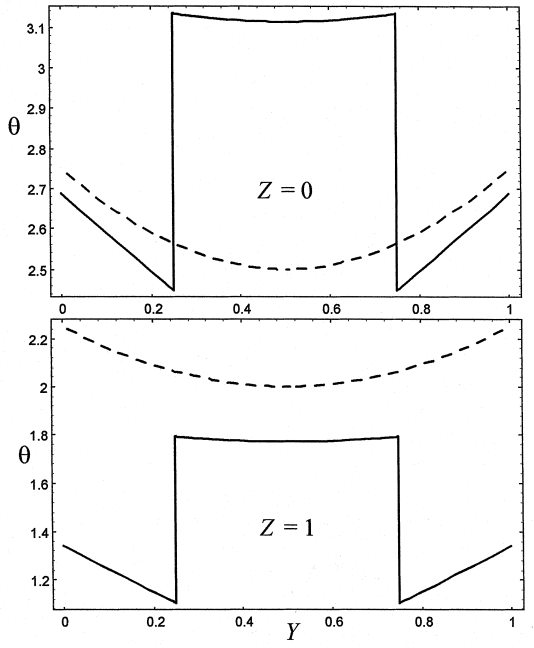

Fig. 10. Plots of θ vs. Y at $Z = 0$ and at $Z = 1$ for $\chi = 0.75$ and $\sigma = 2$. The solid lines refer to $\Xi = 1$, while the dashed lines refer to $\Xi = 0$.

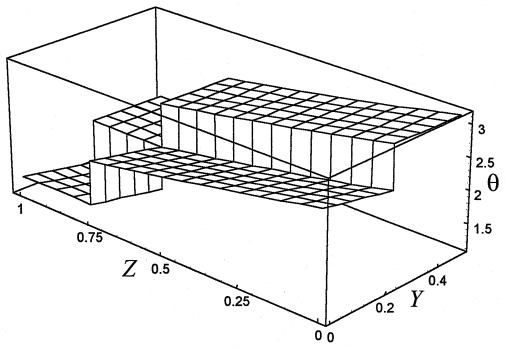

Fig. 9. Plot of the dimensionless temperature θ as a function of Y and Z for $\chi = 0.75$, $\sigma = 2$ and $\Xi = 1$.

Figure 9 refers to $\Xi = 1$ and $\chi = 0.75$. An analysis of this figure shows that four regions can be identified: (a) the region with $0 \leqslant Y \leqslant 0.25$ and $0 \leqslant Z \leqslant 0.75$; (b) the region with $0.25 \leqslant Y \leqslant 0.5$ and $0 \leqslant Z \leqslant 0.75$; (c) the region with $0 \leqslant Y \leqslant 0.25$ and $0.75 \leqslant Z \leqslant 1$; (d) the region with $0.25 \leqslant Y \leqslant 0.5$ and $0.75 \leqslant Z \leqslant 1$. In the region (a), an interference between the wavefronts coming from the planes $Y = 0$ and $Z = 0$ is present. In the region (b), an interference between the wavefronts coming from the planes $Y = 0$, $Y = 1$ and $Z = 0$ occurs. In the region (c), only the temperature signals coming from the plane $Y = 0$ are present. Finally, in the region (d), an

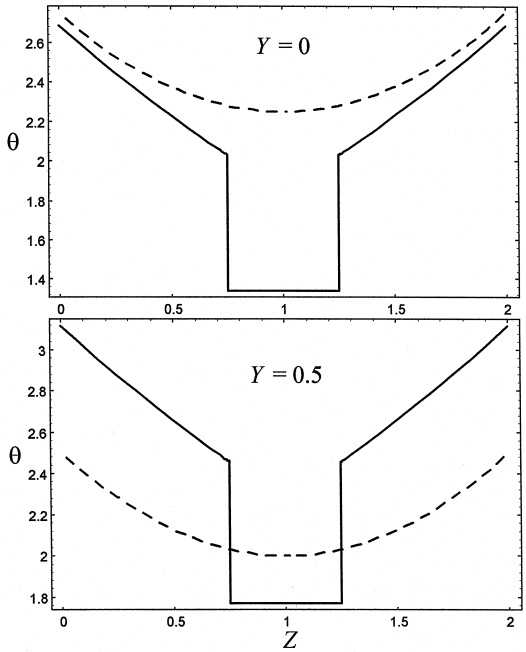

Fig. 11. Plots of θ vs. Z at $Y = 0$ and at $Y = 0.5$ for $\chi = 0.75$ and $\sigma = 2$. The solid lines refer to $\Xi = 1$, while the dashed lines refer to $\Xi = 0$.

interference between the wavefronts coming from the planes $Y = 0$ and $Y = 1$ occurs. Figures 10 and 11 refer to $\chi = 0.75$ and compare the distributions of θ for $\Xi = 1$ and for $\Xi = 0$ on the planes $Z = 0$, $Z = 1$, $Y = 0$ and $Y = 0.5$. In Figs 10 and 11, the interference patterns between the wavefronts, which have been described in the analysis of Fig. 9, can be easily identified.

In Fig. 12, plots of θ vs. χ on the central axis of the bar, i.e. at the position $Y = 0.5$ and $Z = \sigma/2$, are reported for both $\Xi = 1$ and $\Xi = 0$. These plots refer to the interval $0 \leqslant \chi \leqslant 2$ and to three different values of the aspect ratio: $\sigma = 1$, $\sigma = 2$ and $\sigma = 4$. In particular, Fig. 12 shows that the plots for $\Xi = 1$ present discontinuities, which can be explained as follows.

If $\sigma = 1$, θ undergoes two step changes: for $\chi = 0.5$ and for $\chi = 1.5$. The discontinuity for $\chi = 0.5$ is due to the simultaneous arrival of the wavefronts coming from the four boundary planes, while that for $\chi = 1.5$ is due to the arrival of the wavefronts which have been reflected from the boundary planes.

If $\sigma = 2$, θ undergoes three step changes: for $\chi = 0.5$, for $\chi = 1$ and for $\chi = 1.5$. The simultaneous arrival of the wavefronts generated at the boundary planes $Y = 0$ and $Y = 1$ causes the first discontinuity, for $\chi = 0.5$. The arrival of the wavefronts generated at the boundary planes $Z = 0$ and $Z = 2$ is delayed and occurs for $\chi = 1$, in correspondence of the second discontinuity. The third step change, i.e. that for $\chi = 1.5$, is due to the arrival of the wavefronts reflected by the boundary planes $Y = 0$ and $Y = 1$.

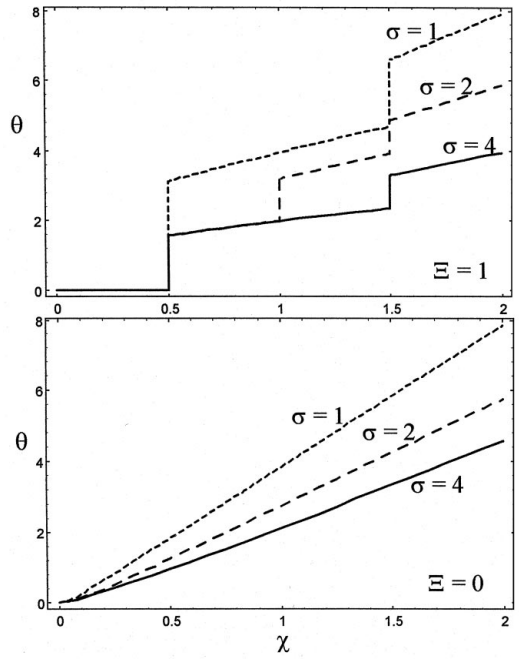

Fig. 12. Plots of θ vs. χ at $Y = 0.5$ and $Z = \sigma/2$ for $\sigma = 1$, $\sigma = 2$ and $\sigma = 4$. The upper frame refers to $\Xi = 1$, while the lower frame refers to $\Xi = 0$.

Finally, if $\sigma = 4$, θ undergoes two step changes: for $\chi = 0.5$ and for $\chi = 1.5$. In the interval $0 \leqslant \chi \leqslant 2$ and for this value of the aspect ratio, no thermal signal which propagates in the Z-direction reaches the central axis, i.e. the position $Y = 0.5$ and $Z = 2$. As a consequence, in the interval $0 \leqslant \chi \leqslant 2$, the time-evolution of θ is influenced only by the thermal waves generated at the boundary planes $Y = 0$ and $Y = 1$. The arrival of the thermal waves coming from these boundary planes causes the discontinuity for $\chi = 0.5$, while the arrival of the waves reflected from these planes causes the discontinuity for $\chi = 1.5$.

An interesting comparison can be made between the behaviour of the temperature field discussed in this section and the behaviour of the temperature field in an infinite solid cylinder whose boundary heat flux undergoes a step change [13]. In both cases, an internal propagation of hyperbolic thermal waves occurs. However, in the case of a solid cylinder, a step change of the boundary heat flux yields a singularity of the temperature field whenever the wavefront created or reflected from the boundary reaches the axis of the cylinder [13]. No such behaviour is detected in the case of a bar with a rectangular cross-section. Indeed, the cylinder with a circular cross-section represents a special geometry, i.e. the axis of the cylinder acts as a focus for the thermal waves coming from the boundary. When a thermal wave with a sharp wavefront reaches the axis of the cylinder, the sharp wavefront focuses on the axis and a singularity occurs. On the contrary, the heat conduction problem examined in the present paper deals with a cylinder having a rectangular cross-section. In this geometry, no point acts as a focus for the thermal waves. As a consequence, the interference between the thermal waves does not yield singularities, even if sharp wavefronts are involved.

7. Conclusions

The hyperbolic heat conduction in a solid bar with a rectangular cross-section and an unsteady boundary heat flux has been analyzed. The heat-flux formulation has been employed. It has been proved that, if a uniform heat flux is prescribed on each boundary plane, the components of the heat flux density can be considered as independent variables. Moreover, each of these components can be determined as the solution of a suitable one-dimensional heat conduction problem. An analytical solution of this one-dimensional problem has been obtained by the Laplace transform method. Then, the temperature field for the three-dimensional propagation of thermal waves induced by arbitrary and unsteady heat fluxes on the six boundary planes has been obtained by employing the local energy-balance equation. Special

attention has been devoted to the case of a bar with insulated end-sections and such that the other boundary planes undergo a step-change of the heat flux density. The interference patterns of the thermal waves have been analyzed for some aspect ratios of the bar cross-section. Finally, a comparison has been performed with the propagation of thermal waves in a solid cylinder having a circular cross-section and subjected to a step-change of the boundary heat flux, studied in ref. [13]. The major difference between the two cases has been emphasized. The circular cross-section causes the axis of the cylinder to be a focus for the thermal waves, while no focus exists in the case of a rectangular cross-section. As a consequence, while thermal waves with sharp wavefronts yield singularities of the temperature field in the case of the circular cylinder, no singularity occurs in the case of the bar with a rectangular cross-section.

Appendix

Function $\tilde{g}(\xi, p, \Lambda)$ can be expressed as

$$\tilde{g}(\xi,p,\Lambda)=\frac{\sinh(\beta\xi)}{p\sinh(\beta)}=\frac{e^{-\beta}}{p}(e^{\beta\xi}-e^{-\beta\xi})\frac{1}{1-e^{-2\beta}}$$
$$=\frac{e^{-\beta}}{p}(e^{\beta\xi}-e^{-\beta\xi})\sum_{n=0}^{\infty}e^{-2n\beta}$$
$$=\sum_{n=0}^{\infty}\left[\frac{e^{-(2n+1-\xi)\beta}}{p}-\frac{e^{-(2n+1+\xi)\beta}}{p}\right]. \tag{A1}$$

On account of equation (A1), the inverse transform $g(\xi, \eta, \Lambda)$ is given by

$$g(\xi,\eta,\Lambda)=\sum_{n=0}^{\infty}\left[\mathscr{L}^{-1}\left\{\frac{e^{-(2n+1-\xi)\beta}}{p}\right\}-\mathscr{L}^{-1}\left\{\frac{e^{-(2n+1+\xi)\beta}}{p}\right\}\right] \tag{A2}$$

where $\mathscr{L}^{-1}$ is the inverse Laplace transform operator. As it can be deduced by employing the tables of Laplace transforms [21], if $\Lambda \neq 0$, the following relation holds

$$f(\omega,\eta,\Lambda)\equiv\mathscr{L}^{-1}\left\{\frac{e^{-\omega\beta}}{p}\right\}=U(\eta-\omega\sqrt{\Lambda})\left[e^{-\omega/(2\sqrt{\Lambda})}+\frac{\omega}{2\sqrt{\Lambda}}\int_{\omega\sqrt{\Lambda}}^{\eta}\frac{e^{-\eta'/(2\Lambda)}}{\sqrt{\eta'^2-\omega^2\Lambda}}I_1\left(\frac{1}{2\Lambda}\sqrt{\eta'^2-\omega^2\Lambda}\right)d\eta'\right] \tag{A3}$$

where U is Heaviside's unit step function and I_v is the modified Bessel function of first kind and order v. On the other hand, in the case $\Lambda = 0$, one obtains [21]

$$f(\omega,\eta,0)\equiv\mathscr{L}^{-1}\left\{\frac{e^{-\omega\sqrt{p}}}{p}\right\}=\operatorname{erfc}\left(\frac{\omega}{2\sqrt{\eta}}\right) \tag{A4}$$

where erfc is the complementary error function. On account of equations (A3) and (A4), equation (A2) can be rewritten as

$$g(\xi,\eta,\Lambda)=\sum_{n=0}^{\infty}[f(2n+1-\xi,\eta,\Lambda)-f(2n+1+\xi,\eta,\Lambda)]. \tag{A5}$$

If $\Lambda \neq 0$, the sum which appears in equations (A5) is not infinite. In fact, as it can be inferred from equations (A3) and (A5), the non-vanishing terms in equation (A5) fulfil the inequality

$$n\leqslant\frac{1}{2}\left(\frac{\eta}{\sqrt{\Lambda}}-1+\xi\right). \tag{A6}$$

Therefore, if $N_{\max}$ is the smallest non-negative integer such that

$$N_{\max}\geqslant\frac{1}{2}\left(\frac{\eta}{\sqrt{\Lambda}}-1+\xi\right) \tag{A7}$$

equation (A5) can be rewritten as

$$g(\xi,\eta,\Lambda)=\sum_{n=0}^{N_{\max}}[f(2n+1-\xi,\eta,\Lambda)-f(2n+1+\xi,\eta,\Lambda)]. \tag{A8}$$

Equations (A7) and (A8) imply that $N_{\max}=0$ and $g(\xi, \eta, \Lambda)=0$ when $\eta<(1-\xi)\Lambda^{1/2}$. If $\Lambda = 0$, equation (A8) can still be employed provided that $N_{\max}=+\infty$.

References

[1] C.C. Ackerman, R.A. Guyer, Temperature pulses in dielectric solids, Annals of Physics 50 (1968) 128–185.
[2] W. Kaminski, Hyperbolic heat conduction for materials with a nonhomogeneous inner structure, ASME Journal of Heat Transfer 112 (1990) 555–560.
[3] K. Mitra, S. Kumar, A. Vedavarz, M.K. Moallemi, Experimental evidence of hyperbolic heat conduction in processed meat, ASME Journal of Heat Transfer 117 (1995) 568–573.
[4] C. Cattaneo, Sulla conduzione del calore, Atti del Seminario Matematico e Fisico dell'Università di Modena 3 (1948) 83–101.
[5] C. Cattaneo, Sur une forme de l'equation de la chaleur éliminant le paradox d'une propagation instantanée, Comptes rendus de l'Académie des Sciences 247 (1958) 431–433.
[6] P. Vernotte, Les paradoxes de la théorie continue de l'équ-

ation de la chaleur, Comptes rendus de l'Académie des Sciences 246 (1958) 3154–3155.
[7] P. Vernotte, La véritable équation de la chaleur, Comptes rendus de l'Académie des Sciences 247 (1958) 2103–2105.
[8] M.N. Özisik, D.Y. Tzou, On the wave theory in heat conduction, ASME Journal of Heat Transfer 116 (1994) 526–535.
[9] H.E. Wilhelm, S.H. Choi, Nonlinear hyperbolic theory of thermal waves in metals, Journal of Chemical Physics 63 (1975) 2119–2123.
[10] A. Barletta, E. Zanchini, Hyperbolic heat conduction and thermal resonances in a cylindrical solid carrying a steady-periodic electric field, International Journal of Heat and Mass Transfer 39 (1996) 1307–1315.
[11] A. Barletta, Hyperbolic propagation of an axisymmetric thermal signal in an infinite solid medium, International Journal of Heat and Mass Transfer 39 (1996) 3261–3271.
[12] A. Barletta, E. Zanchini, Thermal-wave heat conduction in a solid cylinder which undergoes a change of boundary temperature, Heat and Mass Transfer 32 (1997) 285–291.
[13] A. Barletta, B. Pulvirenti, Hyperbolic thermal waves in a solid cylinder with a non-stationary boundary heat flux, International Journal of Heat and Mass Transfer 41 (1998) 107–116.
[14] E. Zanchini, B. Pulvirenti, Periodic heat conduction with relaxation time in cylindrical geometry, Heat and Mass Transfer 33 (1998) 319–326.
[15] H.Q. Yang, Solution of two-dimensional hyperbolic heat conduction by high-resolution numerical methods, Numerical Heat Transfer A 21 (1992) 333–349.
[16] H.-T. Chen, J.-Y. Lin, Analysis of two-dimensional hyperbolic heat conduction problems, International Journal of Heat and Mass Transfer, 37 (1994) 153–164.
[17] H.-T. Chen, J.-Y. Lin, Numerical solution of two-dimensional nonlinear hyperbolic heat conduction problems, Numerical Heat Transfer B 25 (1994) 287–307.
[18] J.I. Frankel, B. Vick, M.N. Özisik, Flux formulation of hyperbolic heat conduction, Journal of Applied Physics 58 (1985) 3340–3345.
[19] M.R. Spiegel, Mathematical Handbook, McGraw-Hill, New York, 1968.
[20] L. Debnath, Integral Transforms and their Applications, 1st ed., Chap. 3, CRC Press, New York, 1995.
[21] G.A. Korn, T.M. Korn, Mathematical Handbook for Scientists and Engineers, McGraw-Hill, New York, 1961, pp. 783–784.